Organic & Biomolecular Chemistry

PAPER

View Article Online
View Journal | View Issue

Open Access Article. Published on 05 novembris 2014. Downloaded on 01.01.2025 01:20:21.
This article is licensed under a Creative Commons Attribution-NonCommercial 3.0 Unported Licence.

Cite this: Org. Biomol. Chem., 2015, 13, 258

Multivalent helix mimetics for PPI-inhibition†

Anna Barnard,[a,b] Jennifer A. Miles,[a,b] George M. Burslem,[a,b] Amy M. Barker[b,c] and Andrew J. Wilson*[a,b]

Received 28th September 2014,
Accepted 5th November 2014

DOI: 10.1039/c4ob02066a

www.rsc.org/obc

The exploitation of multivalent ligands for the inhibition of protein–protein interactions has not yet been explored as a supramolecular design strategy. This is despite the fact that protein–protein interactions typically occur within the context of multi-protein complexes and frequently exploit avidity effects or co-operative binding interactions to achieve high affinity interactions. In this paper we describe preliminary studies on the use of a multivalent *N*-alkylated aromatic oligoamide helix mimetic for inhibition of p53/*h*DM2 and establish that protein dimerisation is promoted, rather than enhanced binding resulting from a higher effective concentration of the ligand.

Introduction

Protein–protein interactions (PPIs) regulate all essential biological processes and are frequently implicated in the development and progression of disease.[1] As targets for molecular recognition, however, PPIs do not conform to conventional models used in drug design in that they are mediated by shallower surfaces with spatially distinct non-covalent contacts rather than the traditional lock and key model of biomolecular protein recognition.[2,3] Therefore, PPIs represent an "ultimate challenge" in terms of complexity for supramolecular design.[4] Several different approaches have been applied that exploit scaffolds that project recognition groups over a large area[5–15] and/or target specific hot-spot residues on the surface.[16,17] A particularly fertile avenue of investigation has concerned the development of secondary structure mimetics;[18] α-helices are the most abundant secondary structure found in proteins and are frequently found at the interface of PPIs.[19] α-Helix mimetics[20–25] are designed to match the spatial arrangement of key binding residues from the helix involved in the interaction.[18] We[26–30] and others[31–33] have developed several types of aromatic oligoamide helix mimetics[34] with the binding groups attached to the 3*O*-,[29,35] 2*O*-[36] and *N*-[30,37] positions on the aromatic building blocks notably for the purposes of p53/*h*DM2 inhibition.[28–30] This PPI is a key regulator of genomic stability and, as such, is of significant interest in the development of cancer treatments.[38,39] p53 binds to *h*DM2 through its helical *N*-terminal transactivation domain. The interaction is mainly controlled by three key 'hot-spot' residues; Phe19, Trp23 and Leu26.[40] *h*DM2 and its partner *h*DMX act as negative regulators by blocking the transcriptional function of p53 and in the case of *h*DM2, through its ubiquitin ligase function which tags p53 for degradation by the proteasome (Fig. 1a).[41] The process by which this occurs at the molecular level is complex, however what is clear is that ubiquitination is promoted by the formation of *h*DM2 homodimers and heterodimers (with *h*DMX), through their respective RING domains.[42] Moreover, a recent study by the Roche group revealed that *h*DM2 and *h*DMX could be induced to form dimers, by a small molecule that spans the p53 binding site of two *h*DM2(X) monomers (Fig. 1b).[43] This inspired the current study – we hypothesized that the use of multivalent[44] helix mimetics might lead to co-operative binding properties either through the avidity resulting from chemically induced dimerisation of the target protein or the higher effective ligand concentration afforded by the proximity of additional covalently tethered copies of the protein-binding ligand (Fig. 1c).[45] Multivalent ligands have been utilised for binding to a multitude of different biological targets including, toxins,[46] heparin,[47] DNA,[48,49] β-tryptase[50] and of particular note for foldamers, amyloid oligomers.[51] Similarly, palindromic ligands have been utilised to inhibit amyloid assembly *e.g.* by stabilizing transthyretin tetramerization[52,53] but not for inhibition of protein–protein interactions (PPIs). Of additional note, a number of dimeric helix mimetics have previously been reported.[54,55] Herein we describe the synthesis of a dimeric *N*-alkylated aromatic oligoamide trimer and illustrate its ability to promote the inhibition of the p53/*h*DM2 interaction by dimerization/aggregation.

[a]School of Chemistry, University of Leeds, Woodhouse Lane, Leeds, LS2 9JT, UK. E-mail: A.J.Wilson@leeds.ac.uk
[b]Astbury Centre for Structural and Molecular Biology, University of Leeds, Woodhouse Lane, Leeds, LS2 9JT, UK
[c]School of Molecular and Cellular Biology, University of Leeds, Woodhouse Lane, Leeds LS2 9JT, UK

†Electronic supplementary information (ESI) available: NMR spectra of compound 2. See DOI: 10.1039/c4ob02066a

This journal is © The Royal Society of Chemistry 2015

Open Access Article. Published on 05 novembris 2014. Downloaded on 01.01.2025 01:20:21.
This article is licensed under a Creative Commons Attribution-NonCommercial 3.0 Unported Licence.

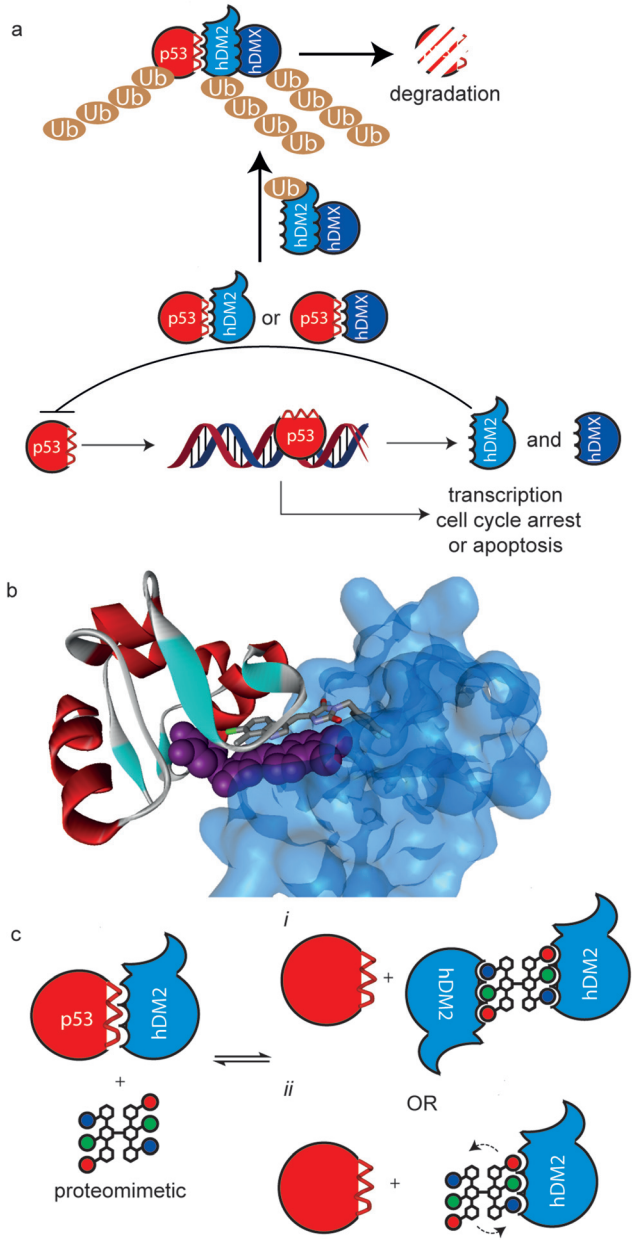

Fig. 1 Multivalent interactions of p53 and *h*DM2 (a) overview of p53 signalling pathway illustrating how *h*DM2(X) dimerisation enhances ubiquitination of p53. (b) X-ray structure of a small molecule inducer of *h*DM2 dimerisation (PDB ID: 3VBG). (c) Schematic depicting possible consequences of multivalent inhibition of p53/*h*DM2 (i) inhibition enhances *h*DM2 dimerization by additional intermolecular *h*DM2 contacts or (ii) proximity of additional ligand enhances affinity through more rapid association upon displacement of bound ligand.

Results and discussion

Synthesis of a divalent oligobenzamide

To obtain a divalent helix mimetic we employed the 'click' chemistry methodology for the synthesis of modified aromatic oligoamides recently reported by our group.[56] A known *N*-alkylated inhibitor **1** of the p53/*h*DM2 interaction possessing phenyl, napthyl and isopropyl side chains to recapitulate the hot-spot residues of p53, was synthesised, functionalised with an alkyne, on solid-phase using an automated microwave peptide synthesiser. Once cleaved from the resin, the trimer was subjected to standard 'click' chemistry reaction conditions with a commercially available ethylene glycol di-azide (Scheme 1). After removal of the copper catalyst, the dimer **2** was isolated in good yield and purity. The equivalent monovalent trimer **1** was also synthesised using previously published methods.[37]

Inhibition of p53/*h*DM2

With the divalent mimetic in hand, we sought to determine if the increased valency would lead to an improvement in the inhibition of the p53/*h*DM2 interaction. We employed a fluorescence anisotropy competition assay whereby increasing concentrations of ligand **1** and **2** were used displace a fluorescein-labelled p53 peptide from the *h*DM2 binding cleft. The observed decrease in anisotropy was used to determine IC_{50} values (Fig. 2). Unfunctionalised monovalent trimer **1** was observed to act as a low μM inhibitor of the p53/*h*DM2 interaction (IC_{50} = 12.3 ± 0.4 μM). When compared against the divalent mimetic **2** a 2-fold improvement in inhibition was observed (IC_{50} = 6.3 ± 0.4 μM). However, as the effective concentration of binding groups is doubled this indicates an absence of positive cooperativity. The most likely cause of such an observation is that dimer **2** simultaneously interacts with two molecules of *h*DM2, but without the benefit of additional intermolecular interactions between the two proteins molecules.

Molecular modelling

To assess if divalent inhibitor **2** was capable of simultaneous interaction with two copies of *h*DM2 we carried out a series of rudimentary modelling experiments. A series of conformers were generated from the structure of mimetic **2**, from which an extended conformation was selected and each copy of the *h*DM2 binding pharmacophore was docked into the binding site of *h*DM2 taken from the crystal structure (Fig. 3). The resultant model indicated no steric clash between the two protein molecules, despite the ethylene glycol linker not adopting a fully extended conformation.

Protein assembly

To obtain experimental evidence of protein assembly we ran a Native PAGE gel (Fig. 4) of *h*DM2 both alone (lane 1) and in the presence of either the monovalent ligand **1** (lanes 2–4) or divalent ligand **2** (lanes 5–7). The gel clearly indicates a difference in the mobility of the protein in the presence of the divalent trimer **2**, consistent with an increase in size. In contrast no such change occurred for monovalent mimetic **1**. We then sought to gain additional more quantitative evidence of protein aggregation. To this end, sedimentation velocity analytical centrifugation (svAUC) was performed on *h*DM2 both with and without DMSO and in the presence of compounds **1** and **2** at a 1 : 4 ratio of protein: ligand (Fig. 5).

In the sample of *h*DM2 alone a clear peak was observed corresponding to the approximate molecular weight of the protein. Importantly, the peak was not perturbed by the pres-

Open Access Article. Published on 05 novembris 2014. Downloaded on 01.01.2025 01:20:21.
This article is licensed under a Creative Commons Attribution-NonCommercial 3.0 Unported Licence.

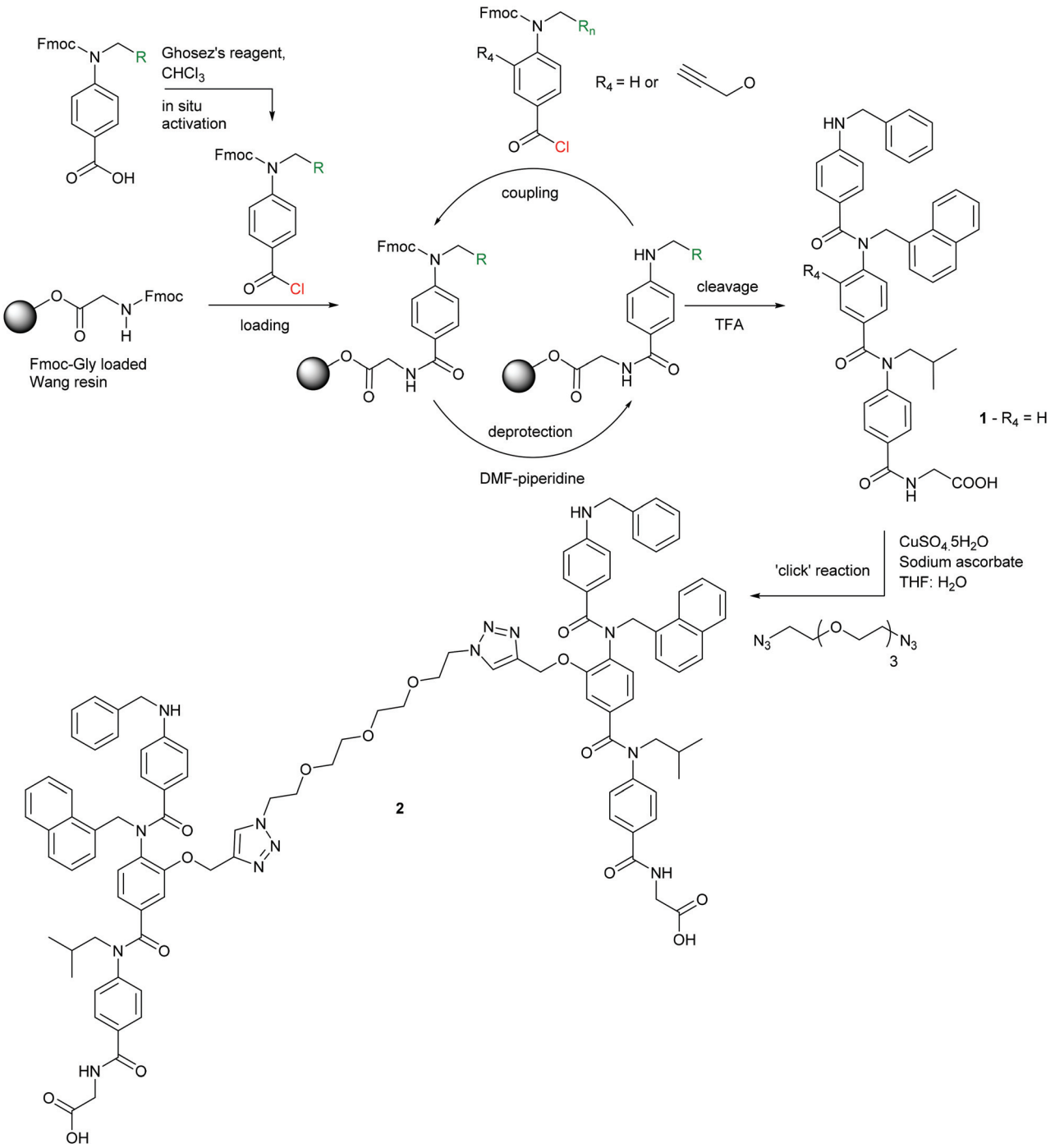

Scheme 1 Synthesis of helix mimetics **1** and **2**.

ence of 5% DMSO, resulting from dilution of the ligand stock solution. When bound to mimetic **1** no significant changes in the overall size or shape of *h*DM2 were observed, a small peak at higher molecular weight also appears however, the majority of the species observed can be assigned as monomeric *h*DM2. The molecular weights were characterised by relating rate of sedimentation and diffusion coefficient to buffer density and the partial specific volume occupied by atoms in solution at a constant temperature, giving peaks as 14.5 kDa and 49.2 kDa for the major and minor peaks. The molecular weight for the major peak is in the region expected for *h*DM2 however the origin of the minor peak is unknown. In the sample containing mimetic **2**, a complete loss of the peak for monomeric *h*DM2 was observed concomitant with the appearance of higher order aggregates. The peak is inconsistent with the mass corresponding to a protein dimer, rather it is the result of a much larger species. It is noteworthy that aggregation by multivalent ligands is not unprecedented[57] and

 This journal is © The Royal Society of Chemistry 2015

Open Access Article. Published on 05 novembris 2014. Downloaded on 01.01.2025 01:20:21.
This article is licensed under a Creative Commons Attribution-NonCommercial 3.0 Unported Licence.

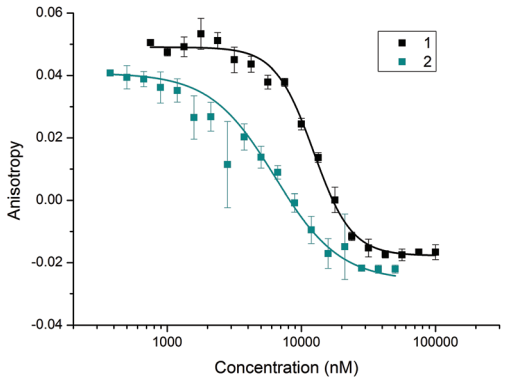

Fig. 2 Fluorescence anisotropy competition curves for the inhibition of the p53/*h*DM2 interaction by the monovalent trimer **1** (black) and the divalent trimer **2** (blue) in assay buffer (40 mM phosphate pH 7.5, 200 mM NaCl, 0.02 mg ml^{-1} BSA). *h*DM2 and FITC-p53 were added to a dilution series of the mimetics to give final concentrations of 154.2 and 54.5 nM, respectively.

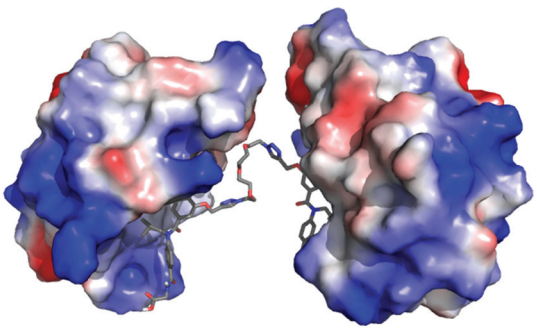

Fig. 3 Molecular modelling of compound **2**; proposed binding mode of compound **2** in the p53 binding cleft of two *h*DM2 molecules (PDB ID: 1YCR).

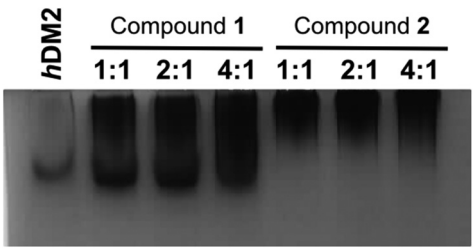

Fig. 4 *h*DM2 analysed by native PAGE in the presence of increasing equivalent of both the monovalent ligand **1** (left) and divalent ligand **2** (right) run in 25 mM Tris buffer pH 8.6, 190 mM glycine. Bands were visualised with Coomassie staining.

this unexpected result will be the focus of future investigations. It is plausible that the dimeric mimetic **2** induces protein dimerisation resulting in a ternary complex that is capable of further aggregation although the possibility that the mimetic is capable of interacting with additional binding sites on *h*DM2 cannot be discounted. Such a scenario, need not necessarily couple to the p53 tracer displacement occurring in the fluorescence anisotropy experiment.

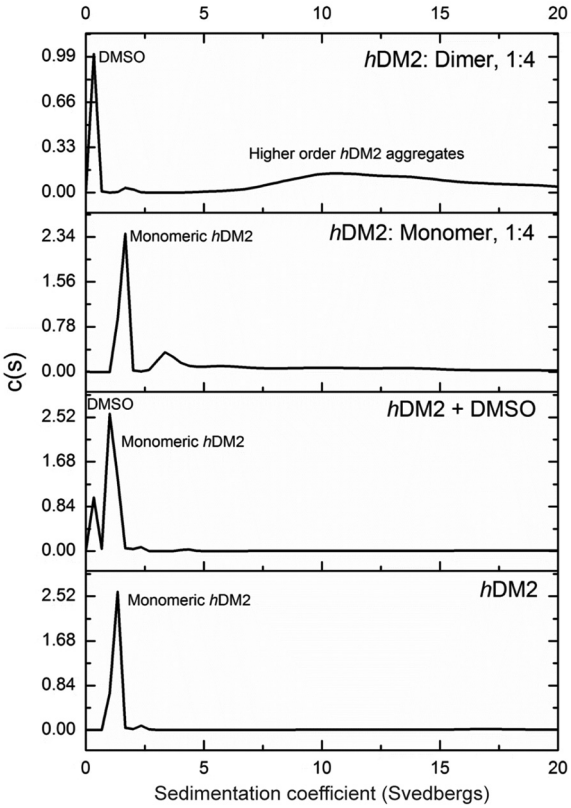

Fig. 5 Analytical ultracentrifugation analysis of *h*DM2 in the presence of monomer **1** and dimer **2** at a 1 : 4 concentration ratio. Samples were prepared in 40 mM phosphate buffer, 200 mM NaCl and 5% DMSO where appropriate. Samples were centrifuged at 48 000 rpm and sedimentation coefficients calculated.

Conclusions

A novel helix mimetic dimer **2** was prepared using 'click' chemistry methodology. This dimeric ligand **2** was found to be a potent inhibitor of the p53/*h*DM2 interaction being twice as potent as the monomeric analogue **1**. When considered in terms of ligand copy number, **1** and **2** are similarly potent. Despite this, more detailed modelling and experimentation revealed the two compounds have differing modes of action. Whilst monomeric ligand **1** favours 1 : 1 stoichiometry with *h*DM2, compound **2** acts as a chemical inducer of dimerization/aggregation. This suggests that, with further refinement, such a strategy could be exploited for protein dimerisation assisted inhibition of protein–protein interactions and in synthetic biology[58] for chemically induced dimerization[59,60] and/or the controlled assembly of proteins.[61,62]

Experimental

General considerations

All chemicals and solvents were purchased and used without further purification. ^{1}H, ^{13}C and 2D NMR spectra were recorded with a Bruker DRX 500 MHz or DPX 300 MHz

Open Access Article. Published on 05 novembris 2014. Downloaded on 01.01.2025 01:20:21.
This article is licensed under a Creative Commons Attribution-NonCommercial 3.0 Unported Licence.

spectrometer. ^{1}H NMR spectra are referenced to residual solvent and chemical shifts are given as parts per million downfield from TMS. Coupling constants are reported to the nearest 0.1 Hz. IR spectra were recorded with a Perkin-Elmer FTIR spectrometer and samples were analysed in the solid phase. Mass spectra (HRMS) were obtained with a Bruker maxis impact 3000 spectrometer using electrospray ionisation. LC-MS experiments were run on a Waters Micromass ZQ spectrometer. Analytical TLC was performed on 0.2 mm silica gel 60 F254 pre-coated aluminium sheets (Merck) and visualised by using UV irradiation. Flash chromatography was carried out on silica gel 60 (35–70 micron particles, Fluoro-Chem). The convention used to assign the spectroscopic data and for naming compounds for this series of aromatic oligoamides has been described previously.[37,56]

Monomer syntheses and the synthesis of the monovalent trimer have been reported previously.

Expression of *h*DM2 and fluorescence anisotropy assays were performed as described previously.[36,56]

Synthesis of *N*-(*N*-(*N*-(benzyl-4-aminobenzoyl)-*N*-naphth-1-yl-4-aminobenzoyl)-*N*-isobutyl-4-aminobenzoyl)-glycine dimer

Glycine-loaded Wang resin (254 mg, 0.2 mmol) was swelled in anhydrous DMF (5 ml) 15 minutes prior to reaction. The monomers; benzyl (450 mg, 1.0 mmol), alkyne-1-naphthyl (554 mg, 1.0 mmol) and isobutyl (415 mg, 1.0 mmol) were each dissolved in anhydrous $CHCl_3$ (10 ml) and pre-activated for coupling with Ghosez's reagent (630 μl, 20% in $CHCl_3$, 0.96 mmol) for 1 hour at room temperature. The coupling reactions were carried out on a CEM Liberty™ microwave assisted automated peptide synthesiser. The trimer was then cleaved from the resin with TFA–DCM (1 : 1, 1 ml) and analysed by LC-MS to confirm formation of the desired trimer. The trimer (25.7 mg, 0.033 mmol) was dissolved in THF–H_2O (1 : 1, 10 ml) and 1,11-diazido-3,6-9-trioxaundecance (3.47 μl, 0.017 mmol) was added followed by $CuSO_4{\cdot}5H_2O$ (0.42 mg, 1.6×10^{-3} mmol) and sodium ascorbate (0.43 mg, 3.3×10^{-3} mmol). The reaction mixture was stirred overnight at room temperature. The solvent was then removed and the residue taken up in DMSO (5 ml) and any copper precipitate removed by centrifugation. The DMSO was then removed under high vacuum affording the desired compound as a sticky orange solid (13.2 mg, 7.36×10^{-3} mmol, 43%). R_f = 0.3 (3 : 2, DCM–MeOH); ^{1}H NMR (500 MHz, DMSO-d_6) δ: 8.14–8.12 (m, 2–3°-*T*, 2H), 7.91–7.69 (br m, ArC*H*, 5H), 7.47–7.45 (m, ArC*H*, 4H), 7.27–7.05 (m, ArC*H*, 23H), 6.92–6.90 (m, 1-*H*2, 4H), 6.42–6.28 (m, 2-*H*5, 2-*H*6, 1-*H*3, 8H), 4.86–4.84 (s, 2-*Hα*, 4H), 4.55–4.53 (s, 1-N*H*, 2H), 4.26–4.24 (s, 4-*Hα*, 4H), 3.84–3.83 (s, 1-*Hα*, 4H), 3.64 (s, 3-*Hα*, 4H), 3.55–3.41(m, 2–3°-*Hβ*, 2–3°-*Hγ*, 2–3°-*Hθ*, 2–3°-*Hι*, 8H), 3.23 (s, 2–3°-*Hδ*, 2–3°-*Hε*, 2–3°-*Hζ*, 2–3°-*Hη*, 8H), 1.72–1.69 (m, 3-*Hβ*, 2H), 0.84 (s, 3-*Hγ*, 12H); HRMS: Calcd $[M + H]^+$ ($C_{104}H_{105}N_{14}O_{15}$) *m*/*z* = 1789.787835, Found $[M + H]^+$ *m*/*z* = 1789.785716; ν_{max} (cm^{-1}): 3319s (O–H), 2916s (C–H), 1635s (C═O), 1601s (C═O), 1504s, 1418m, 1385m, 1338w, 1284s, 1182m, 1130s, 1017s.

Molecular modelling

The protein structure for *h*DM2 (PDB ID: 1YCR) was prepared using the protein preparation wizard within Maestro (Schrodinger) and the docking grid prepared by selecting the binding groove of the p53 helix using Glide (Schrodinger).

The monovalent inhibitor was docked using Glide (Schrodinger) and these docked structures superimposed onto a low energy structure of the divalent inhibitor to provide a model of protein dimerization.

Native PAGE

Protein samples were separated on a 10% acrylamide native PAGE gel in 25 mM Tris, 190 mM glycine buffer pH 8.6, gel was run at 25 mA. Bands were visualised with Coomassie staining. Samples were diluted from 10 mM DMSO stocks into 50 mM Tris buffer pH 8.0, 200 mM NaCl, 0.5 mM DTT.

Sedimentation velocity analytical ultracentrifugation

Samples (0.32 ml) were placed in a 1.2 cm pathlength 2-sector meniscus-matching epon centrepiece cell constructed with sapphire windows and centrifuged at 48 000 rpm in an An50-Ti rotor in an Optima XL-I analytical ultracentrifuge at 20.0 °C. Changes in concentration of the solute were detected by interference optics, with a total of 500 scans being taken over approximately 8.3 hours. Buffer densities and viscosities were calculated by Sednterp version 1.09, omitting the presence of 5% DMSO.[63] Radial interference profiles were fitted using the program Sedfit version 12.1b using a continuous distribution c(S) Lamm equation model.[64]

Acknowledgements

This work was supported by the European Research Council [ERC-StG-240324].

Notes and references

1 O. Keskin, A. Gursoy, B. Ma and R. Nussinov, *Chem. Rev.*, 2008, **108**, 1225–1244.
2 M. R. Arkin and J. A. Wells, *Nat. Rev. Drug Discovery*, 2004, **3**, 301–317.
3 L.-G. Milroy, T. N. Grossmann, S. Hennig, L. Brunsveld and C. Ottmann, *Chem. Rev.*, 2014, **114**, 4695–4748.
4 A. J. Wilson, *Chem. Soc. Rev.*, 2009, **38**, 3289–3300.
5 P. B. Crowley, P. Ganji and H. Ibrahim, *ChemBioChem*, 2008, **9**, 1029–1033.
6 A. Ojida, M.-a. Inoue, Y. Mito-oka, H. Tsutsumi, K. Sada and I. Hamachi, *J. Am. Chem. Soc.*, 2006, **128**, 2052–2058.
7 Y. Mito-oka, S. Tukiji, T. Hiraoka, N. Kasagi, S. Shinkai and I. Hamachi, *Tetrahedron Lett.*, 2001, **42**, 7059–7062.
8 H. Bayraktar, P. S. Ghosh, V. M. Rotello and M. J. Knapp, *Chem. Commun.*, 2006, 1390–1392.
9 J. Ohkanda, R. Satoh and N. Kato, *Chem. Commun.*, 2009, 6949–6951.

 This journal is © The Royal Society of Chemistry 2015

Open Access Article. Published on 05 novembris 2014. Downloaded on 01.01.2025 01:20:21.
This article is licensed under a Creative Commons Attribution-NonCommercial 3.0 Unported Licence.

10 J. Muldoon, A. E. Ashcroft and A. J. Wilson, *Chem. – Eur. J.*, 2010, **16**, 100–103.
11 A. J. Wilson, J. Hong, S. Fletcher and A. D. Hamilton, *Org. Biomol. Chem.*, 2007, **5**, 276–285.
12 L. K. Tsou, C.-H. Chen, G. E. Dutschman, Y.-C. Cheng and A. D. Hamilton, *Bioorg. Med. Chem. Lett.*, 2012, **22**, 3358–3361.
13 B. A. Rosenzweig, N. T. Ross, M. J. Adler and A. D. Hamilton, *J. Am. Chem. Soc.*, 2010, **132**, 6749–6754.
14 Y. Cheng, L. K. Tsou, J. Cai, T. Aya, G. E. Dutschman, E. A. Gullen, S. P. Grill, A. P.-C. Chen, B. D. Lindenbach, A. D. Hamilton and Y.-c. Cheng, *Antimicrob. Agents Chemother.*, 2010, **54**, 197–206.
15 D. Margulies, Y. Opatowsky, S. Fletcher, I. Saraogi, L. K. Tsou, S. Saha, I. Lax, J. Schlessinger and A. D. Hamilton, *ChemBioChem*, 2009, **10**, 1955–1958.
16 D. Bier, R. Rose, K. Bravo-Rodriguez, M. Bartel, J. M. Ramirez-Anguita, S. Dutt, C. Wilch, F.-G. Klärner, E. Sanchez-Garcia, T. Schrader and C. Ottmann, *Nat. Chem.*, 2013, **5**, 234–239.
17 R. i. E. McGovern, H. Fernandes, A. R. Khan, N. P. Power and P. B. Crowley, *Nat. Chem.*, 2012, **4**, 527–533.
18 V. Azzarito, K. Long, N. S. Murphy and A. J. Wilson, *Nat. Chem.*, 2013, **5**, 161–173.
19 B. N. Bullock, A. L. Jochim and P. S. Arora, *J. Am. Chem. Soc.*, 2011, **133**, 14220–14223.
20 B. B. Lao, K. Drew, D. A. Guarracino, T. F. Brewer, D. W. Heindel, R. Bonneau and P. S. Arora, *J. Am. Chem. Soc.*, 2014, **136**, 7877–7888.
21 S. Kushal, B. B. Lao, L. K. Henchey, R. Dubey, H. Mesallati, N. J. Traaseth, B. Z. Olenyuk and P. S. Arora, *Proc. Natl. Acad. Sci. U. S. A.*, 2014, **111**, 7531–7536.
22 P. Ravindranathan, T.-K. Lee, L. Yang, M. M. Centenera, L. Butler, W. D. Tilley, J.-T. Hsieh, J.-M. Ahn and G. V. Raj, *Nat. Commun.*, 2013, **4**, 1923.
23 W. E. Martucci, J. M. Rodriguez, M. A. Vargo, M. Marr, A. D. Hamilton and K. S. Anderson, *MedChemComm*, 2013, **4**, 1247–1256.
24 A. Kazi, J. Sun, K. Doi, S.-S. Sung, Y. Takahashi, H. Yin, J. M. Rodriguez, J. Becerril, N. Berndt, A. D. Hamilton, H.-G. Wang and S. d. M. Sebti, *J. Biol. Chem.*, 2011, **286**, 9382–9392.
25 I. Saraogi, J. A. Hebda, J. Becerril, L. A. Estroff, A. D. Miranker and A. D. Hamilton, *Angew. Chem., Int. Ed.*, 2010, **49**, 736–739.
26 G. M. Burslem, H. F. Kyle, A. L. Breeze, T. A. Edwards, A. Nelson, S. L. Warriner and A. J. Wilson, *ChemBioChem*, 2014, **15**, 1083–1087.
27 P. Prabhakaran, A. Barnard, N. S. Murphy, C. A. Kilner, T. A. Edwards and A. J. Wilson, *Eur. J. Org. Chem.*, 2013, 3504–3512.
28 V. Azzarito, P. Prabhakaran, A. I. Bartlett, N. S. Murphy, M. J. Hardie, C. A. Kilner, T. A. Edwards, S. L. Warriner and A. J. Wilson, *Org. Biomol. Chem.*, 2012, **10**, 6469–6472.
29 J. P. Plante, T. Burnley, B. Malkova, M. E. Webb, S. L. Warriner, T. A. Edwards and A. J. Wilson, *Chem. Commun.*, 2009, 5091–5093.
30 F. Campbell, J. P. Plante, T. A. Edwards, S. L. Warriner and A. J. Wilson, *Org. Biomol. Chem.*, 2010, **8**, 2344–2351.
31 A. Shaginian, L. Whitby, S. Hong, I. Hwang, B. Farooqi, M. Searcey, J. Chen, P. Vogt and D. Boger, *J. Am. Chem. Soc.*, 2009, **131**, 5564–5572.
32 T.-K. Lee and J.-M. Ahn, *ACS Comb. Sci.*, 2010, **13**, 107–111.
33 J. T. Ernst, J. Becerril, H. S. Park, H. Yin and A. D. Hamilton, *Angew. Chem., Int. Ed.*, 2003, **42**, 535–539.
34 G. M. Burslem and A. J. Wilson, *Synlett*, 2014, 324–335.
35 N. S. Murphy, P. Prabhakaran, V. Azzarito, J. P. Plante, M. J. Hardie, C. A. Kilner, S. L. Warriner and A. J. Wilson, *Chem. – Eur. J.*, 2013, **19**, 5546–5550.
36 V. Azzarito, P. Prabhakaran, A. I. Bartlett, N. S. Murphy, M. J. Hardie, C. A. Kilner, T. A. Edwards, S. L. Warriner and A. J. Wilson, *Org. Biomol. Chem.*, 2012, **10**, 6469–6472.
37 K. Long, T. A. Edwards and A. J. Wilson, *Bioorg. Med. Chem.*, 2013, **21**, 4034–4040.
38 K. K. Hoe, C. S. Verma and D. P. Lane, *Nat. Rev. Drug Discovery*, 2014, **13**, 217–236.
39 K. Khoury, G. M. Popowicz, T. A. Holak and A. Domling, *MedChemComm*, 2011, **2**, 246–260.
40 P. H. Kussie, S. Gorina, V. Marechal, B. Elenbaas, J. Moreau, A. J. Levine and N. P. Pavletich, *Science*, 1996, **274**, 948–953.
41 L. K. Linares, A. Hengstermann, A. Ciechanover, S. Müller and M. Scheffner, *Proc. Natl. Acad. Sci. U. S. A.*, 2003, **100**, 12009–12014.
42 K. Linke, P. D. Mace, C. A. Smith, D. L. Vaux, J. Silke and C. L. Day, *Cell Death Differ.*, 2008, **15**, 841–848.
43 B. Graves, T. Thompson, M. Xia, C. Janson, C. Lukacs, D. Deo, P. Di Lello, D. Fry, C. Garvie, K.-S. Huang, L. Gao, C. Tovar, A. Lovey, J. Wanner and L. T. Vassilev, *Proc. Natl. Acad. Sci. U. S. A.*, 2012, **109**, 11788–11793.
44 M. Mammen, S. K. Choi and G. M. Whitesides, *Angew. Chem., Int. Ed.*, 1998, **37**, 2755–2794.
45 A. Barnard and D. K. Smith, *Angew. Chem., Int. Ed.*, 2012, **51**, 6572–6581.
46 E. Fan, Z. Zhang, W. E. Minke, Z. Hou, C. L. M. J. Verlinde and W. G. J. Hol, *J. Am. Chem. Soc.*, 2000, 2663–2664.
47 A. C. Rodrigo, A. Barnard, J. Cooper and D. K. Smith, *Angew. Chem., Int. Ed.*, 2011, **50**, 4675–4679.
48 P. Posocco, S. Pricl, S. Jones, A. Barnard and D. K. Smith, *Chem. Sci.*, 2010, **1**, 393–404.
49 A. Barnard, P. Posocco, S. Pricl, M. Calderon, R. Haag, M. E. Hwang, V. W. T. Shum, D. W. Pack and D. K. Smith, *J. Am. Chem. Soc.*, 2011, **133**, 20288–20300.
50 P. R. Wich and C. Schmuck, *Angew. Chem., Int. Ed.*, 2010, **49**, 4113–4116.
51 L. Fülöp, I. M. Mándity, G. Juhász, V. Szegedi, A. Hetényi, E. Wéber, Z. Bozsó, D. Simon, M. Benkő, Z. Király and T. A. Martinek, *PLoS One*, 2012, **7**, e39485.
52 N. S. Green, S. K. Palaninathan, J. C. Sacchettini and J. W. Kelly, *J. Am. Chem. Soc.*, 2003, **125**, 13404–13414.
53 S. E. Kolstoe, P. P. Mangione, V. Bellotti, G. W. Taylor, G. A. Tennent, S. Deroo, A. J. Morrison, A. J. A. Cobb, A. Coyne, M. G. McCammon, T. D. Warner, J. Mitchell,

Open Access Article. Published on 05 novembris 2014. Downloaded on 01.01.2025 01:20:21.
This article is licensed under a Creative Commons Attribution-NonCommercial 3.0 Unported Licence.

R. Gill, M. D. Smith, S. V. Ley, C. V. Robinson, S. P. Wood and M. B. Pepys, *Proc. Natl. Acad. Sci. U. S. A.*, 2010, **107**, 20483–20488.

54 M. K. P. Jayatunga, S. Thompson and A. D. Hamilton, *Bioorg. Med. Chem. Lett.*, 2014, **24**, 717–724.

55 O. V. Kulikov, S. Thompson, H. Xu, C. D. Incarvito, R. T. W. Scott, I. Saraogi, L. Nevola and A. D. Hamilton, *Eur. J. Org. Chem.*, 2013, 3433–3445.

56 A. Barnard, K. Long, D. J. Yeo, J. A. Miles, V. Azzarito, G. M. Burslem, P. Prabhakaran, T. A. Edwards and A. J. Wilson, *Org. Biomol. Chem.*, 2014, **12**, 6794–6799.

57 C. Sisu, A. J. Baron, H. M. Branderhorst, S. D. Connell, C. A. G. M. Weijers, R. de Vries, E. D. Hayes, A. V. Pukin, M. Gilbert, R. J. Pieters, H. Zuilhof, G. M. Visser and W. B. Turnbull, *ChemBioChem*, 2009, **10**, 329–337.

58 E. H. C. Bromley, K. Channon, E. Moutevelis and D. N. Woolfson, *ACS Chem. Biol.*, 2008, **3**, 38–50.

59 M. Skwarczynska, M. Molzan and C. Ottmann, *Proc. Natl. Acad. Sci. U. S. A.*, 2013, **110**, E377–E386.

60 E. M. Hobert and A. Schepartz, *J. Am. Chem. Soc.*, 2012, **134**, 3976–3978.

61 E. N. Salgado, X. I. Ambroggio, J. D. Brodin, R. A. Lewis, B. Kuhlman and F. A. Tezcan, *Proc. Natl. Acad. Sci. U. S. A.*, 2010, **107**, 1827–1832.

62 K. Oohora, S. Burazerovic, A. Onoda, Y. M. Wilson, T. R. Ward and T. Hayashi, *Angew. Chem., Int. Ed.*, 2012, **51**, 3818–3821.

63 H. Durchschlag, in *Thermodynamic data for biochemistry and biotechnology*, ed. H.-J. Hinz, Springer-Verlag, Berlin, Editon edn, 1986, pp. 45–182.

64 P. Schuck, *Biophys. J.*, 2000, **78**, 1606–1619.

This journal is © The Royal Society of Chemistry 2015